Geophysical Research Letters

Supporting Information for

Effect of Regional Marine Cloud Brightening on Climate Tipping Elements

Haruki Hirasawa[1], Dipti Hingmire[1], Hansi Singh[1], Philip J. Rasch[2], Peetak Mitra[3,4]

[1]School of Earth and Ocean Sciences, University of Victoria, Victoria, BC, Canada

[2]Department of Atmospheric Sciences, University of Washington, Seattle, WA, USA

[3]Palo Alto Research Center, Palo Alto, CA, USA

[4]Excarta, San Fransisco, CA, USA

Contents of this file

Introduction

Here, we present supporting information for "Effect of Regional Marine Cloud Brightening on Climate Tipping Elements". In Text S1, we discuss our choice of tipping elements to analyse and general caveats around the assessment of tipping points using earth system models. In Texts S2 to S10, we describe the metrics for each tipping elements and sources for each metric definition. In Figure S1, we compare the CDNC perturbation effect used herein to sea salt emission simulations with similar forcings. In Figure S2, we display the time series of the TEMs in the analysis period for historical, SSP2-4.5, and MCB simulations to show the rate of the baseline GHG impacts on each to contextualize the MCB impacts. In Figure S3 we show the absolute TEM changes for SSP2-4.5 and each SSP2-4.5+MCB simulation relative to the historical period. In Table 1, we summarize the tipping element metrics used in this study.

Text S1. Climate tipping element metrics

We assess the MCB impact on tipping elements by computing the change in 14 selected tipping element metrics (TEMs) in our CESM2 simulations (Table S1), based on supplementary discussion from a recent synthesis paper (Armstrong McKay et al., 2022). We choose to omit the Arctic winter sea ice collapse and East Antarctic icesheet collapse as the minimum bounds

on the tipping thresholds in each case exceed 4°C, well above the warming seen in SSP2-4.5 for CESM2. For the other tipping points, the lower bounds on the threshold of warming at which tipping occurs falls within the range of warming seen in SSP2-4.5 (up to ~3°C). Additionally, we omit mountain glacier and boreal forest/tundra tipping elements, as there are we are not able to evaluate the joint influence of temperature and precipitation changes in these cases.

These TEMs are not direct measures of tipping point risk. However, they are proximal indicators of the tendency of climate change impacts on each tipping point. We note that some of the tipping points considered herein are not possible in CESM2 due to missing process representation (such as icesheet height changes) or occur on time scales and at warming levels not captured in our 50-year SSP2-4.5 simulations. Furthermore, CESM2 has substantial biases in key fields related to each tipping point, which likely introduces errors in each, compounding with uncertainties in the large-scale climate response.

Text S2. North American (a) and Eurasian (e) permafrost area

We compute the areal extent of North American (60N to 75N; 160W to 60W) and Eurasian (60N to 80N; 65E to 180E) boreal permafrost, defined as land model grid points where the annual minimum soil ice concentration > 0 at 3.5m for the present and prior year. This is the definition of (Slater & Lawrence, 2013), except we use the land model's soil ice concentration rather than soil temperature < 0C, though this has little effect in the resulting permafrost area. Abrupt regional permafrost thaw is hypothesized to be a result of localized feedback processes (Schuur et al., 2015), which may occur across a region in a short period of time. However, such processes are difficult to represent on ESM spatial scales (Lawrence et al., 2019) and CESM2 projects substantial but linear losses in permafrost area under SSP2-4.5.

Text S3. Greenland warming (b)

We compute annual mean 2-metre temperature over Greenland (60N to 80N; 60W to 20W) to assess the possible MCB impact on the surface elevation feedback, wherein icesheet thinning due to melt causes additional warming and further melt (Crowley & Baum, 1995; Robinson et al., 2012), as surface melt is the principle driver of Greenland ice sheet loss (Joughin et al., 2012; Pattyn et al., 2018). However, we do not use a CESM2 configuration with two-way coupling between the Greenland ice sheet and atmosphere. Thus, the surface elevation feedback does not operate in our simulations and the temperature changes in the model may be underestimated.

Text S4. North Atlantic Gyre (c) and Atlantic Meridional Overturning (h)

We compute the Annual mean AMOC index (Cheng et al., 2013) as a measure of overturning strength and North Atlantic (45N to 60N; 50W to 20W) area-mean annual maximum mixed layer depth as a measure of ocean convection strength (Swingedouw et al., 2021). These are two related tipping metrics associated with potential tipping elements in the Atlantic Ocean circulation. CESM2 overestimates present day AMOC strength by 2-3 Sv (Danabasoglu et al., 2020) and experiences a rapid, but linear decline in AMOC index over the SSP2-4.5 simulation (Fig. S2). CESM2 has lower North Atlantic subpolar gyre stratification than observed (Swingedouw et al., 2021), and thus may have a too-sensitive convection response.

Text S5. Barents winter sea ice (d)

We compute Barents (70N to 80N; 10E to 60E) Sea March April sea ice area (the winter sea ice maximum), which may rapidly transition into a year-round ice free state under sufficient warming (Drijfhout et al., 2015; Eisenman & Wettlaufer, 2009). Regional winter sea ice collapse may occur in regions like the Barents Sea (Armstrong McKay et al., 2022), though we do not see winter sea ice collapse the region in CESM2 under SSP2-4.5 (Fig. S2). Furthermore, CESM2 generally underestimates present day Arctic sea ice extent (Danabasoglu et al., 2020), which may indicate sea ice is too sensitive to warming in the model (Kay et al., 2021; Massonnet et al., 2018).

Text S6. Amazon water deficit (g)

CESM2 does not include dynamic vegetation biogeography (Lawrence et al., 2019). Thus, we cannot directly assess vegetation change in the model. Instead, for the Amazon and Sahel, we assume the tipping elements are principally driven by changes in hydroclimate and assess changes in precipitation and evaporation in the regions. In the case of the Amazon, we estimate MCB effect of possible Amazon rainforest dieback using the area-mean (7S to 7N; 70W to 45W) maximum climatological water deficit (MCWD) defined as the most negative value of the cumulative precipitation minus evaporation over a year (Malhi et al., 2009). MCWD and annual precipitation together can be used to classify vegetation type in the Amazon (Malhi et al., 2009), and changes in the hydroclimate could trigger dieback of the rainforest. Additionally, CESM2 has a substantial dry bias in the Amazon (Danabasoglu et al., 2020), which introduces uncertainty in the precipitation response to forcing in the region.

Text S7. Sahel rainfall (i)

In the case of the Sahel (10N to 20N; 15W to 35E), we simply assess the regional mean, annual mean precipitation, which is an indicator of West African monsoon strength. It is thought that vegetation-albedo feedback could rapidly increase monsoon strength and vegetation cover in the region, as occurred in the Green Sahara period (Hopcroft & Valdes, 2021; Pausata et al., 2020). There is substantial inter-model uncertainty regarding the greenhouse gas impact on the Sahel (Monerie et al., 2020). Though we consider Sahel greening a risk of GHG/MCB forcing here, some have argued for geoengineering via large-scale afforestation wherein greening is considered desirable (Pausata et al., 2020).

Text S8. Amundsen sea zonal wind speed (k)

We focus our evaluation of the MCB impacts on West Antarctic ice sheets by focusing on Thwaites glacier stability. Here we assume marine ice sheet instability due to grounding lines reaching retrograde slopes is the principle tipping point (Feldmann & Levermann, 2015; Joughin et al., 2012; Pattyn et al., 2018). Marine ice sheet melt is principally driven by circumpolar deep water flow into the vicinity of the ice sheets (Jenkins et al., 2018), which is correlated with wind stress and zonal wind speed in the Amundsen sea off the coast of West Antarctica (Fogwill et al., 2014; Holland et al., 2019). Thus, we use Pine Island/Thwaites Troughs (71.8S to 70.2S; 115W to 102W) area-mean annual mean zonal wind speed to estimate the GHG/MCB effect on West Antarctic ice sheet melt following (Holland et al., 2019). Our CESM2 experiments do not

include two-way coupling to ice sheet dynamics; thus, we cannot directly assess ice sheet changes. Furthermore, the averaging box is derived from observational conditions, and thus may not be suitable for CESM2, which is coarser resolution and has different sea ice distribution in the region compared to observed.

Text S9. East Antarctic Westerly position (l)

Though less certain than West Antarctic icesheet loss, there is modeling and observational evidence that portions of the East Antarctic ice sheet such as in the Wilkes basin (Fogwill et al., 2014; Mengel & Levermann, 2014) could collapse, with a central warming threshold estimate of 3°C (Armstrong McKay et al., 2022). We evaluate the potential atmospheric circulation impacts on the ice sheet by computing the southern hemisphere extratropical surface westerly jet position, as southward shifts of the jet are associated with increased bottom water transport and basal melt (Fogwill et al., 2014). This is defined as the latitude of the zonally averaged (0 to 180E) surface zonal wind maximum.

Text S10. Coral heat stress (f,j,m,n)

We consider the impact of GHG/MCB forcing on coral reefs in four regions (Caribbean Sea - 12N to 25N; 85W to 65W, West Indian Ocean - 25S to 0; 35E to 60E, West Tropical Pacific Ocean - 10S to 10N; 100E to 150E, Coral Sea - 25S to 10S; 145E to 165E) by computing changes in the area-mean annual maximum degree heating weeks (DHW) (Liu et al., 2003). DHW is the cumulative weekly anomaly above a threshold equal to maximum monthly mean temperature over a reference period (1990-1999) of historical CESM2 plus 1C in a twelve-week window. Severe heat stress is considered to occur if DHW > 8 C·weeks (Latham et al., 2013; Liu et al., 2003). Here we simply assess the change in annual maximum DHW as a measure of the mean intensity of summertime hot conditions in a region.

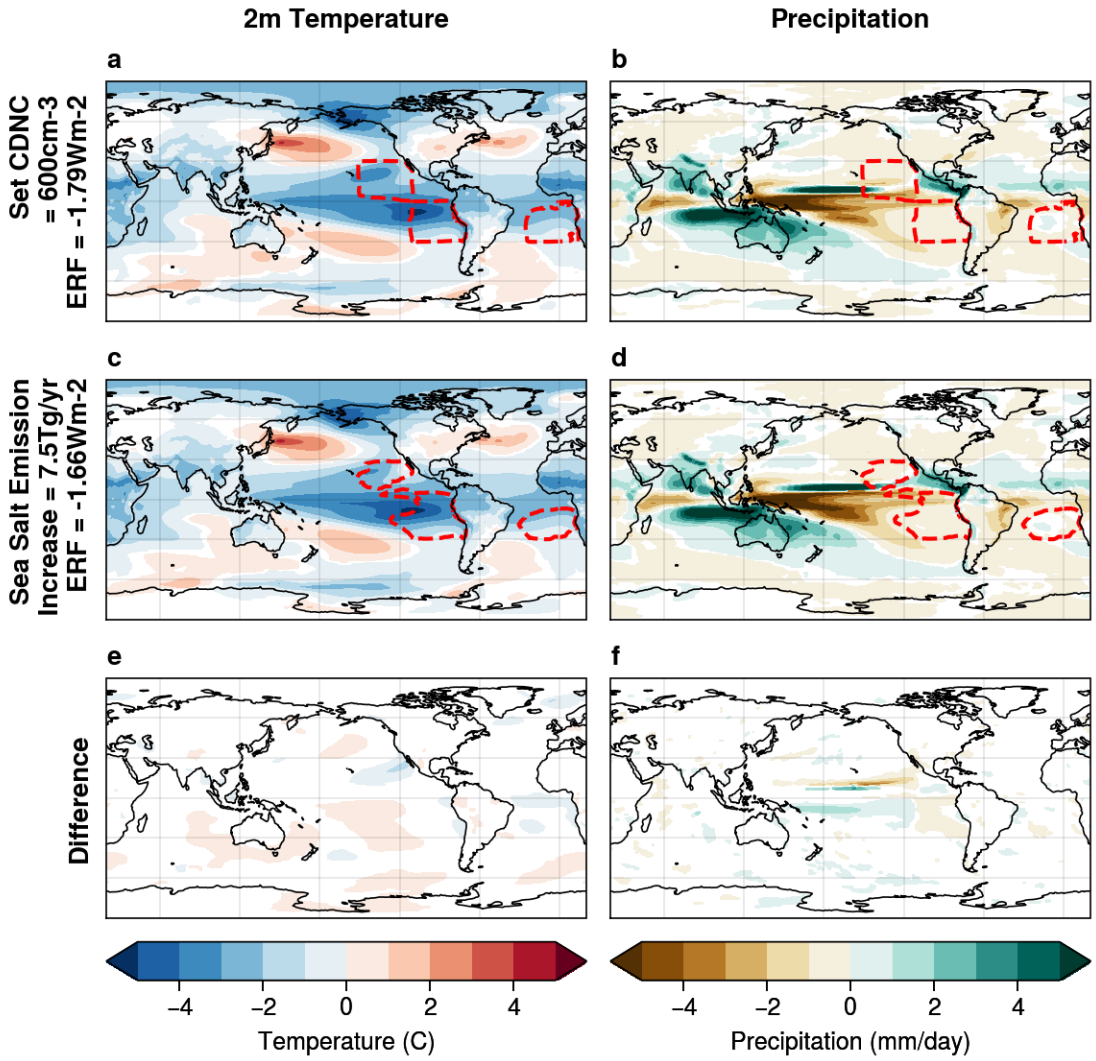

Figure S1. Annual mean temperature (a,c,e) and precipitation (b,d,f) anomalies relative to SSP2-4.5 for 2025-2049. Top row (a,b) shows anomalies when CDNC=600cm^{-3} is applied in NEP, SEP, and SEA. Middle row (c,d) shows anomalies in a simulation with SSP2-4.5 baseline conditions wherein accumulation mode sea salt emissions are increased by 2.5Tg/yr in each region NEP, SEP, and SEA (thus 7.5Tg/yr globally). This emission value was selected as it results in global mean forcing approximately the same as the CDNC simulation. Bottom row (e,f) shows the difference between the two. Non-significant signals are masked in white. Regions where all-sky top-of-atmosphere radiative anomalies exceed 10Wm^{-2} in the corresponding fixed-SST time-slice simulations are shown with red contours in (a,b,c,f) to display any differences in the locations of the forcings caused by CDNC versus sea salt emission perturbations.

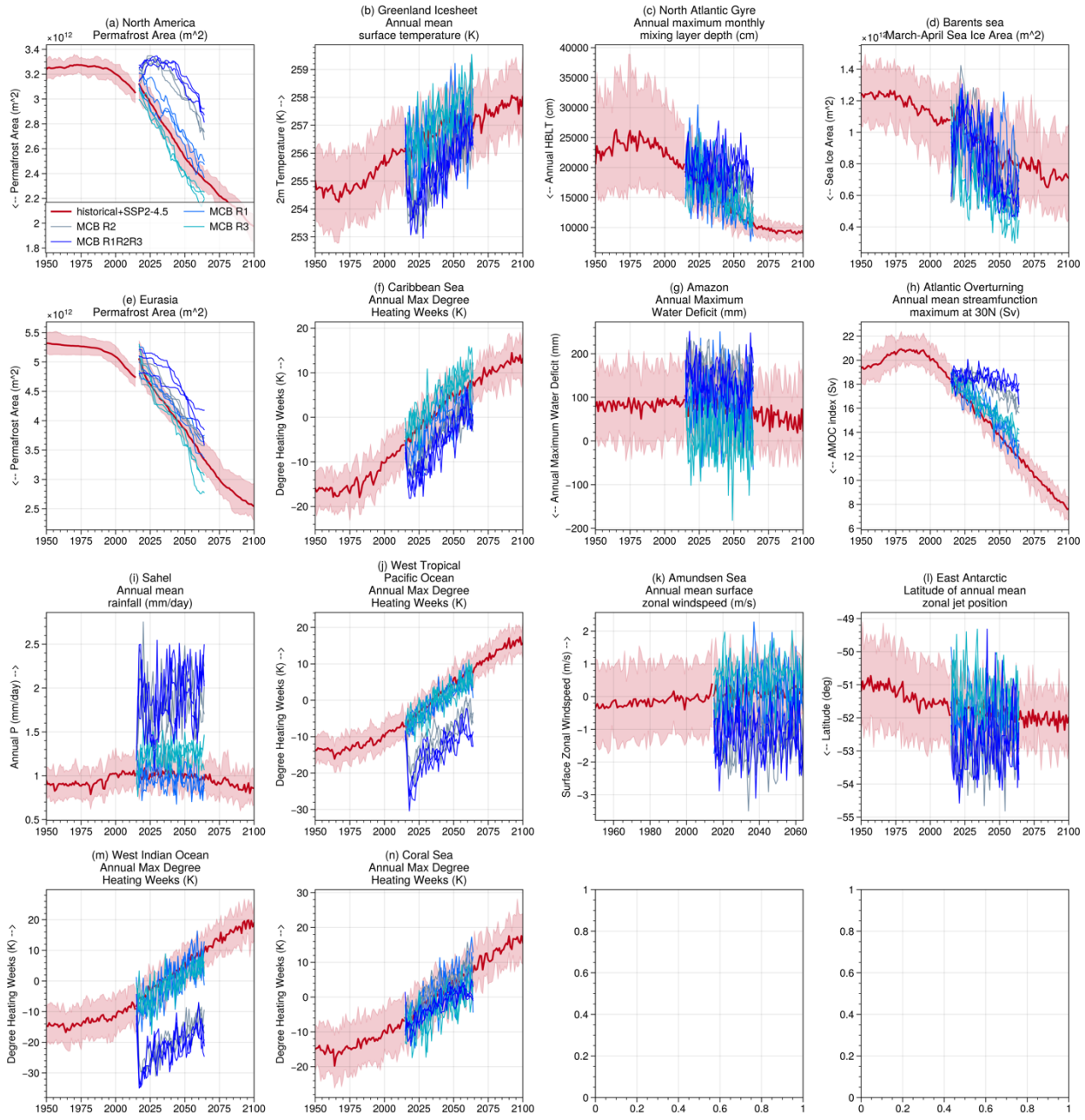

Figure S2. Time series of Tipping point metric changes for historical and SSP2-4.5 (red), SSP2-4.5 + ALL MCB (navy blue), SSP2-4.5 + NEP MCB (medium blue), SSP2-4.5 + SEP MCB (grey blue), and SSP2-4.5 SEA MCB (turquoise blue). Solid red line indicates ensemble average and red shading indicates 5 to 95 percentile range. Arrows in y-labels indicate the direction of increased tipping point risk.

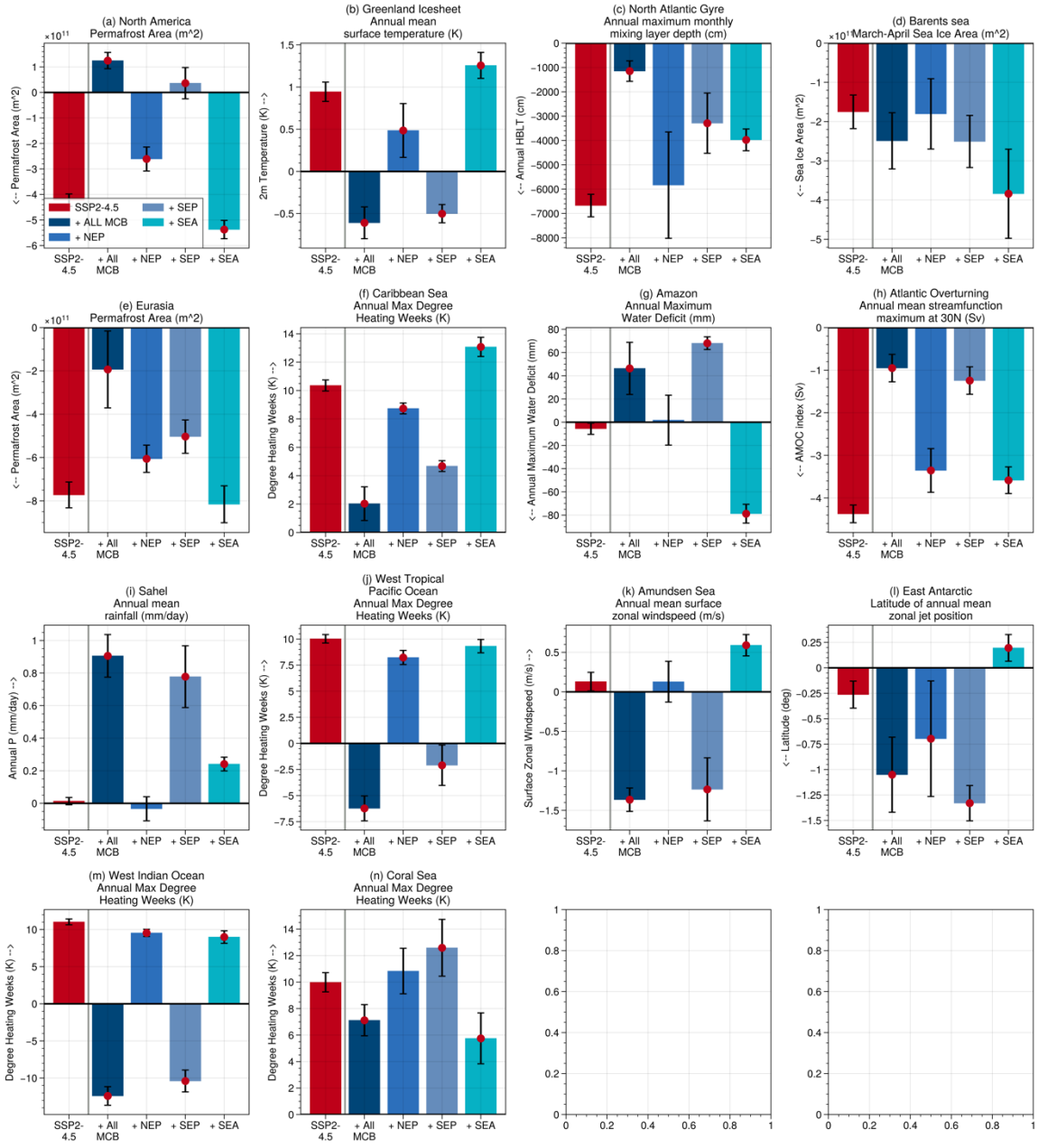

Figure S3. Bar plots displaying anomalies in the 14 selected tipping element metrics for each simulation relative to the historical baseline. In each panel, 2036-2046 anomalies relative to historical 2000-2010 anomalies are displayed from left to right for SSP2-4.5 (red), SSP2-4.5 + ALL MCB (navy blue), SSP2-4.5 + NEP MCB (medium blue), SSP2-4.5 + SEP MCB (grey blue), and SSP2-4.5 SEA MCB (turquoise blue). We show the anomalies relative to historical for the MCB simulations, such that a zero anomaly means MCB returns the tipping element metric to its historical state. Error bars show the 5-95 percentile range (computed as 1.96 times the standard error) and red dots indicate cases where the SSP2-4.5 + MCB anomaly is significantly different from the SSP2-4.5 anomaly by Student's t-test (i.e., the MCB impact is significant). Arrows in y-labels indicate the direction of increased tipping point risk.

Table S1. Summary of climate tipping point metrics assessed in Fig. 3, S1, and S2.

Fig. 3 Label	Tipping Point	Metric	Citation
d	Barents Sea winter sea ice	March-April sea ice area (70N to 80N; 10E to 60E)	(Drijfhout et al., 2015)
b	Greenland icesheet	Annual mean 2m temperature (land; 60N to 80N; 60W to 20W)	(Crowley & Baum, 1995; Robinson et al., 2012)
h	Atlantic Meridional Overturning	Annual mean Atlantic meridional streamfunction maximum at 30N	(Cheng et al., 2013; Swingedouw et al., 2021)
c	North Atlantic Gyre	Annual maximum mixed layer depth (ocean; 45N to 60N; 50W to 20W)	(Sgubin et al., 2017; Swingedouw et al., 2021)
a	North American Permafrost	Land area where annual minimum soil ice concentration > 0 at 3.5m for two consecutive years (land; 60N to 75N; 160W to 60W)	(Lawrence et al., 2012; Slater & Lawrence, 2013)
e	Eurasian Permafrost	Land area where annual minimum soil ice concentration \> 0 at 3.5m for two consecutive years (land; 60N to 80N; 65E to 180E)	(Lawrence et al., 2012; Slater & Lawrence, 2013)
h	Amazon water deficit	Annual maximum water deficit (land; 7S to 7S; 70W to 45W)	(Malhi et al., 2009)
i	Sahel rainfall	Annual mean precipitation (land; 10N to 20N; 15W to 35E)	(Hopcroft & Valdes, 2021; Pausata et al., 2020)
k	Amundsen sea windspeed	Annual mean Amundsen sea surface zonal wind speed (ocean; 71.8S to 70.2S; 115W to 102W)	(Holland et al., 2019)
l	East Antarctic Westerly position	Latitude of local maximum annual and zonal mean surface zonal wind speed (zonal mean over 80S to 40S; 0 to 180W)	(Fogwill et al., 2014)
f	Caribbean Sea coral heat stress	Annual maximum degree heating weeks (ocean; 12N to 25N; 85W to 65W)	(Liu et al., 2003)
m	West Indian Ocean coral heat stress	Annual maximum degree heating weeks (ocean; 25S to 0; 35E to 60E)	(Liu et al., 2003)
j	West Tropical Pacific coral heat stress	Annual maximum degree heating weeks (ocean; 10S to 10N; 100E to 150E)	(Liu et al., 2003)
n	Coral Sea coral heat stress	Annual maximum degree heating weeks (ocean; 25S to 10S; 145E to 165E)	(Liu et al., 2003)

Armstrong McKay, D. I., Staal, A., Abrams, J. F., Winkelmann, R., Sakschewski, B., Loriani, S., Fetzer, I., Cornell, S. E., Rockström, J., & Lenton, T. M. (2022). Exceeding 1.5°C global warming could trigger multiple climate tipping points. *Science*, *377*, 6611. https://doi.org/10.1126/science.abn7950

Cheng, W., Chiang, J. C. H., & Zhang, D. (2013). Atlantic Meridional Overturning Circulation (AMOC) in CMIP5 Models: RCP and Historical Simulations. *Journal of Climate*, *26*(18), 7187–7197. https://doi.org/10.1175/JCLI-D-12-00496.1

Crowley, T. J., & Baum, S. K. (1995). Is the Greenland Ice Sheet bistable? *Paleoceanography*, *10*(3), 357–363. https://doi.org/10.1029/95PA00662

Danabasoglu, G., Lamarque, J. -F., Bacmeister, J., Bailey, D. A., DuVivier, A. K., Edwards, J., Emmons, L. K., Fasullo, J., Garcia, R., Gettelman, A., Hannay, C., Holland, M. M., Large, W. G., Lauritzen, P. H., Lawrence, D. M., Lenaerts, J. T. M., Lindsay, K., Lipscomb, W. H., Mills, M. J., … Strand, W. G. (2020). The Community Earth System Model Version 2 (CESM2). *Journal of Advances in Modeling Earth Systems*, *12*(2). https://doi.org/10.1029/2019MS001916

Drijfhout, S., Bathiany, S., Beaulieu, C., Brovkin, V., Claussen, M., Huntingford, C., Scheffer, M., Sgubin, G., & Swingedouw, D. (2015). Catalogue of abrupt shifts in Intergovernmental Panel on Climate Change climate models. *Proceedings of the National Academy of Sciences*, *112*(43). https://doi.org/10.1073/pnas.1511451112

Eisenman, I., & Wettlaufer, J. S. (2009). Nonlinear threshold behavior during the loss of Arctic sea ice. *Proceedings of the National Academy of Sciences*, *106*(1), 28–32. https://doi.org/10.1073/pnas.0806887106

Feldmann, J., & Levermann, A. (2015). Collapse of the West Antarctic Ice Sheet after local destabilization of the Amundsen Basin. *Proceedings of the National Academy of Sciences*, *112*(46), 14191–14196. https://doi.org/10.1073/pnas.1512482112

Fogwill, C. J., Turney, C. S. M., Meissner, K. J., Golledge, N. R., Spence, P., Roberts, J. L., England, M. H., Jones, R. T., & Carter, L. (2014). Testing the sensitivity of the East Antarctic Ice Sheet to Southern Ocean dynamics: Past changes and future implications: SENSITIVITY OF THE EAST ANTARCTIC ICE SHEET TO SOUTHERN OCEAN DYNAMICS. *Journal of Quaternary Science*, *29*(1), 91–98. https://doi.org/10.1002/jqs.2683

Holland, P. R., Bracegirdle, T. J., Dutrieux, P., Jenkins, A., & Steig, E. J. (2019). West Antarctic ice loss influenced by internal climate variability and anthropogenic forcing. *Nature Geoscience*, *12*(9), 718–724. https://doi.org/10.1038/s41561-019-0420-9

Hopcroft, P. O., & Valdes, P. J. (2021). Paleoclimate-conditioning reveals a North Africa land–atmosphere tipping point. *Proceedings of the National Academy of Sciences*, *118*(45), e2108783118. https://doi.org/10.1073/pnas.2108783118

Jenkins, A., Shoosmith, D., Dutrieux, P., Jacobs, S., Kim, T. W., Lee, S. H., Ha, H. K., & Stammerjohn, S. (2018). West Antarctic Ice Sheet retreat in the Amundsen Sea driven by decadal oceanic variability. *Nature Geoscience*, *11*(10), 733–738. https://doi.org/10.1038/s41561-018-0207-4

Joughin, I., Alley, R. B., & Holland, D. M. (2012). Ice-Sheet Response to Oceanic Forcing. *Science*, *338*(6111), 1172–1176. https://doi.org/10.1126/science.1226481

Kay, J. E., DeRepentigny, P., Holland, M. M., Bailey, D. A., DuVivier, A. K., Blanchard-Wrigglesworth, E., Deser, C., Jahn, A., Singh, H. A., Smith, M. M., Webster, M. A., Edwards, J., Lee, S.-S., Rodgers, K., & Rosenbloom, N. A. (2021). *Less surface sea ice melt in the CESM2 improves Arctic sea ice simulation with minimal non-polar climate impacts* [Preprint]. Climatology (Global Change). https://doi.org/10.1002/essoar.10507477.1

Latham, J., Kleypas, J., Hauser, R., Parkes, B., & Gadian, A. (2013). Can marine cloud brightening reduce coral bleaching?: Can marine cloud brightening reduce coral bleaching? *Atmospheric Science Letters*, *14*(4), 214–219. https://doi.org/10.1002/asl2.442

Lawrence, D. M., Fisher, R. A., Koven, C. D., Oleson, K. W., Swenson, S. C., Bonan, G., Collier, N., Ghimire, B., van Kampenhout, L., Kennedy, D., Kluzek, E., Lawrence, P. J., Li, F., Li, H., Lombardozzi, D., Riley, W. J., Sacks, W. J., Shi, M., Vertenstein, M., … Zeng, X. (2019). The Community Land Model Version 5: Description of New Features, Benchmarking, and Impact of Forcing Uncertainty. *Journal of Advances in Modeling Earth Systems*, *11*(12), 4245–4287. https://doi.org/10.1029/2018MS001583

Lawrence, D. M., Slater, A. G., & Swenson, S. C. (2012). Simulation of Present-Day and Future Permafrost and Seasonally Frozen Ground Conditions in CCSM4. *Journal of Climate*, *25*(7), 2207–2225. https://doi.org/10.1175/JCLI-D-11-00334.1

Liu, G., Strong, A. E., & Skirving, W. (2003). Remote sensing of sea surface temperatures during 2002 Barrier Reef coral bleaching. *Eos, Transactions American Geophysical Union*, *84*(15), 137–141. https://doi.org/10.1029/2003EO150001

Malhi, Y., Aragão, L. E. O. C., Galbraith, D., Huntingford, C., Fisher, R., Zelazowski, P., Sitch, S., McSweeney, C., & Meir, P. (2009). Exploring the likelihood and mechanism of a climate-change-induced dieback of the Amazon rainforest. *Proceedings of the National Academy of Sciences*, *106*(49), 20610–20615. https://doi.org/10.1073/pnas.0804619106

Massonnet, F., Vancoppenolle, M., Goosse, H., Docquier, D., Fichefet, T., & Blanchard-Wrigglesworth, E. (2018). Arctic sea-ice change tied to its mean state through thermodynamic processes. *Nature Climate Change*, *8*(7), 599–603. https://doi.org/10.1038/s41558-018-0204-z

Mengel, M., & Levermann, A. (2014). Ice plug prevents irreversible discharge from East Antarctica. *Nature Climate Change*, *4*(6), 451–455. https://doi.org/10.1038/nclimate2226

Monerie, P.-A., Wainwright, C. M., Sidibe, M., & Akinsanola, A. A. (2020). Model uncertainties in climate change impacts on Sahel precipitation in ensembles of CMIP5 and CMIP6 simulations. *Climate Dynamics*, *55*(5–6), 1385–1401. https://doi.org/10.1007/s00382-020-05332-0

Pattyn, F., Ritz, C., Hanna, E., Asay-Davis, X., DeConto, R., Durand, G., Favier, L., Fettweis, X., Goelzer, H., Golledge, N. R., Kuipers Munneke, P., Lenaerts, J. T. M., Nowicki, S., Payne, A. J., Robinson, A., Seroussi, H., Trusel, L. D., & Van Den Broeke, M. (2018). The Greenland and Antarctic ice sheets under 1.5 °C global warming. *Nature Climate Change*, *8*(12), 1053–1061. https://doi.org/10.1038/s41558-018-0305-8

Pausata, F. S. R., Gaetani, M., Messori, G., Berg, A., Maia de Souza, D., Sage, R. F., & deMenocal, P. B. (2020). The Greening of the Sahara: Past Changes and Future Implications. *One Earth*, *2*(3), 235–250. https://doi.org/10.1016/j.oneear.2020.03.002

Robinson, A., Calov, R., & Ganopolski, A. (2012). Multistability and critical thresholds of the Greenland ice sheet. *Nature Climate Change*, *2*(6), 429–432. https://doi.org/10.1038/nclimate1449

Schuur, E. A. G., McGuire, A. D., Schädel, C., Grosse, G., Harden, J. W., Hayes, D. J., Hugelius, G., Koven, C. D., Kuhry, P., Lawrence, D. M., Natali, S. M., Olefeldt, D., Romanovsky, V. E., Schaefer, K., Turetsky, M. R., Treat, C. C., & Vonk, J. E. (2015). Climate change and the permafrost carbon feedback. *Nature*, *520*(7546), 171–179. https://doi.org/10.1038/nature14338

Sgubin, G., Swingedouw, D., Drijfhout, S., Mary, Y., & Bennabi, A. (2017). Abrupt cooling over the North Atlantic in modern climate models. *Nature Communications*, *8*(1), 14375. https://doi.org/10.1038/ncomms14375

Slater, A. G., & Lawrence, D. M. (2013). Diagnosing Present and Future Permafrost from Climate Models. *Journal of Climate*, *26*(15), 5608–5623. https://doi.org/10.1175/JCLI-D-12-00341.1

Swingedouw, D., Bily, A., Esquerdo, C., Borchert, L. F., Sgubin, G., Mignot, J., & Menary, M. (2021). On the risk of abrupt changes in the North Atlantic subpolar gyre in CMIP6 models. *Annals of the New York Academy of Sciences*, *1504*(1), 187–201. https://doi.org/10.1111/nyas.14659